Surface plasmons in a metal nanowire coupled to colloidal quantum dots: Scattering properties and quantum entanglement

Guang-Yin Chen, Neill Lambert, Chung-Hsien Chou, Yueh-Nan Chen, and Franco Nori

Phys. Rev. B **84**, 045310 — Published 13 July 2011

DOI: 10.1103/PhysRevB.84.045310

Surface Plasmons in a Metal Nanowire Coupled to Colloidal Quantum Dots: Scattering Properties and Quantum Entanglement

Guang-Yin Chen,[1,2] Neill Lambert,[2] Chung-Hsien Chou,[1] Yueh-Nan Chen,[1,*] and Franco Nori[2,3]

[1] *Department of Physics and National Center for Theoretical Sciences, National Cheng-Kung University, Tainan 701, Taiwan*

[2] *Advanced Science Institute, RIKEN, Wako-shi, Saitama 351-0198, Japan*

[3] *Physics Department, University of Michigan, Ann Arbor, MI 48109-1040, USA*

(Dated: April 6, 2011)

We investigate coherent single surface-plasmon transport in a metal nanowire strongly coupled to two colloidal quantum dots. Analytical expressions are obtained for the transmission and reflection coefficients by solving the corresponding eigenvalue equation. Remote entanglement of the wave functions of the two quantum dots can be created if the inter-dot distance is equal to a multiple half-wavelength of the surface plasmon. Furthermore, by applying classical laser pulses to the quantum dots, the entangled states can be stored in metastable states which are decoupled from the surface plasmons.

PACS numbers: 03.67.Bg, 42.50.Ex, 73.20.Mf, 73.21.La

I. INTRODUCTION

Colloidal quantum dots (QDs) are fluorescent core-shell semiconductor nanocrystals with tunable luminescence properties (e.g., broad excitation spectra, narrow emission spectra, and size-dependent emission), which have recently attracted much attention for their ability to act as photon detectors[1].

When a light wave strikes a metal surface, it can excite a surface-plasmon-polariton: a surface electromagnetic wave coupled to plasma oscillations. Recently, the concept of plasmonics, in analogy to photonics, has received much attention since surface plasmons (SPs) reveal strong analogies to light propagation in conventional dielectric components[2–4]. For example, it is now possible to confine them to subwavelength dimensions[5] leading to novel approaches for waveguiding below the diffraction limit[6]. The combination of subwavelength confinement, single-mode operation, and the relatively low-power propagation loss of SP polaritons could be used to miniaturize existing photonic circuits[7]. Furthermore, the strong coupling between SP and emitters[8] can be utilized to enhance infrared photodetectors[9], the fluorescence of QDs[10], and light transmission through metal nanoarrays[11]. High-field surface plasmon confinement was also used to demonstrate an all-optical modulator[12], to provide an extra degree of freedom for information storage[13], and to estimate the reflectivity of structures or surface roughness[14].

In a related context, advances in quantum information science have promoted an experimental drive for physical realizations of highly-entangled states[15]. Successes have been obtained within quantum-optical and atomic systems[15]. However, due to scalability requirements, solid-state realizations of such phenomena are promising[16–18]. Furthermore, while initial attention has been focused on the coupling between nearby qubits with local interactions[19–21], entangling arbitrary pairs of remote qubits is still an important goal. Circuit quantum electrodynamics (QED), for example, is one promising candidate to couple two distant qubits via a cavity bus[19,22].

Motivated by these recent developments in plasmonics and quantum information science, we propose a novel scheme that can entangle two remote QDs coupled to a metal nanowire. The idea is inspired by recent experiments showing single surface plasmons in metallic nanowires coupled to QDs[23]. We use a real-space Hamiltonian[24] to treat the coherent surface-plasmon transport in the wire coupled to two dots. The transmission and reflection spectra of SPs for both single QD and double QDs cases in the *non-linear* quadratic dispersion regime (which occurs near the vicinity of the band edge) has been studied in our previous work[25]. In that work the scattering spectra reveals a Fano resonance due to the interference between localized and delocalized SP channels. Here, we focus on a different goal (the entanglement generated through the scattering of SPs) in a different regime: the *linear* dispersion regime, instead of the non-linear regime. In the limit of infinite Purcell factor, $P \to \infty$, we find that maximally entangled states can be created if the separation between the two dots is equal to an integer multiple half-wavelength of the optical plasmon. Furthermore, we show the entangled state information can also be stored in metastable states, which are decoupled from the surface plasmons, by separately applying classical laser pulses to each QD. The storage efficiency of the entangled states is equal to $(1 - 1/P)$.

A similar scheme was also recently proposed independently in Ref. [26,27], who solved a similar setup using a master equation description of the two quantum dots. Their findings are consistent with our results, with the maximum of the concurrence occurring at the same values of the dot distance. Furthermore, they show the concurrence behavior as a function of time, for a single initial excitation, which illustrates that indeed the concurrence exists on an experimentally accessible time-

scale. The approaches used are very different: we use a real-space scattering formulation, in contrast with their master equation. We stress that the reflection and transmission coefficients computed here can be directly accessed experimentally, which is not easy to do by other methods. Furthermore, we have considered the important effects of Ohmic loss. Moreover, we propose a way to store the entanglement produced in this manner.

II. PLASMON SCATTERED BY TWO QUANTUM DOTS

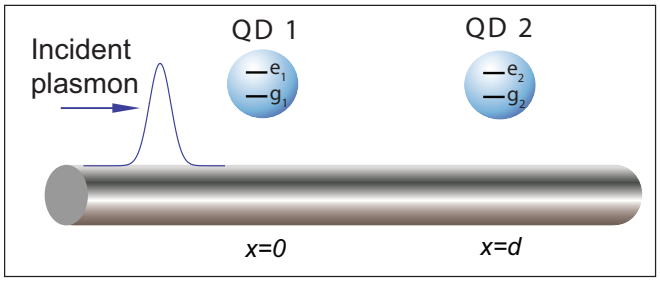

FIG. 1: (Color online) Schematic diagram of a metal nanowire coupled to two QDs. A single surface plasmon injected from the left is coherently scattered by the dots.

When a colloidal semiconductor QD is placed close to a metal nanowire, a strong coupling between the QD exciton and SP can occur[28–30], as in traditional cavity QED[31]. As shown in Fig. 1, the system we consider here is composed of two nominally identical QDs, both with energy spacing $\hbar\omega_0$, separated a distance d, near a cylindrical metal nanowire. We assume that a surface plasmon emitted from a source QD is incident from the left with energy $E_k = v_g k$. Here, v_g and k are the group velocity and wavevector of the incident SP, respectively. Since the SP is propagating on the surface of the metal nanowire, it inevitably suffers from dissipation (such as Ohmic loss). As a result, the source of the incoming plasmon (e.g. an additional QD) must be placed close to the first QD to minimize the initial losses (i.e. those which occur before the plasmon reaches the two-dot region). We also propose a practical way to further minimize all the dissipation affects in the next section.

Following the method proposed in Refs. [32,33], we write an effective non-Hermitian Hamiltonian for the combined quantum-dot plasmon system (where the dissipation has been included as an imaginary energy),

$$\begin{aligned} H = &\sum_{j=1,2} \hbar\left[\omega_0 - i\left(\frac{\Gamma'}{2}\right)\right]\sigma_{e_j,e_j} + \int dk\ \hbar v_g|k| a_k^\dagger a_k \\ &-\hbar g\int dk\ \left[\left(\sigma_+^{(1)} + \sigma_+^{(2)} e^{ikd}\right) a_k + \text{h.c.}\right] \\ &-i\hbar\frac{\sin(k_0 d)}{2k_0 d}\gamma_0\left(\sigma_+^{(1)}\sigma_-^{(2)} + \sigma_-^{(1)}\sigma_+^{(2)}\right), \end{aligned} \tag{1}$$

where $\sigma_{e_j,e_j} = |e_j\rangle\langle e_j|$ represents the diagonal element and $\sigma_+^{(j)} = |e_j\rangle\langle g_j|$ represents the off-diagonal of the j-th QD operator, and $a_k^\dagger$ is the creation operator of the surface plasmon. Here, $k_0 = \omega_0/v_g$, and g is the coupling constant between the excitons and SP. The term in the last line,

$$\Gamma^{\text{SR}} = \left[\frac{i\sin(k_0 d)}{2(k_0 d)}\right]\gamma_0, \tag{2}$$

is the contribution from the collective decay (Super-Radiance, hence the super-index "SR") effect[34], with γ_0 being the exciton decay rate into free space, and

$$\Gamma' \equiv \gamma_0 + \Gamma_0, \tag{3}$$

is the total dissipation including the decay rate into free space γ_0 and other dissipative channels (for example, the Ohmic loss) Γ_0. We can include the Ohmic loss of plasmons during the scattering process in this way because a loss of the plasmon is equivalent to a lose of the excitation in the quantum dots. In addition,

$$\delta \equiv \frac{E_k}{\hbar} - \omega_0, \tag{4}$$

is the detuning between the incident SP energy with E_k and the QD exciton energy ω_0.

The validity of this non-Hermitian form relies on the fact that Γ' is small and that we only consider one excitation. Hence we do not need to consider the effect of the quantum jump terms one usually needs for a full description of the system[33,35]. However, this implies that there is a certain time scale of decay of the highly-entangled state into other modes, even if they are not emitted into the surface-plasmonic environment (though typically the Purcell factor is large, so emission into SPs will dominate any decay process). This reinforces the need to transfer the fragile entangled state to a metastable state.

Since we are only interested in the case where the incident SP is nearly-resonant with the two QDs, we can rewrite $\int dk\ \hbar v_g|k| a_k^\dagger a_k$ as $\int dk\ \hbar v_g k(a_{R,k}^\dagger a_{R,k} + a_{L,k}^\dagger a_{L,k})$ and $(\sigma_+^{(1)} + \sigma_+^{(2)} e^{ikd})a_k$ as $(\sigma_+^{(1)} + \sigma_+^{(2)} e^{ikd})(a_{R,k} + a_{L,k})$. Transforming Eq. (1) into real space, one obtains

$$\begin{aligned} H = \hbar\int dx\Big\{ &-iv_g c_R^\dagger(x)\frac{\partial}{\partial x}c_R(x) + iv_g c_L^\dagger(x)\frac{\partial}{\partial x}c_L(x) \\ &+\hbar g\sum_{j=1,2}\delta(x-(j-1)d)\left[c_R^\dagger(x)\sigma_-^{(j)} + c_R(x)\sigma_+^{(j)}\right. \\ &\left.+c_L^\dagger(x)\sigma_-^{(j)} + c_L(x)\sigma_+^{(j)}\right]\Big\} + \sum_{j=1,2}\hbar\left[\omega_0 - i\left(\frac{\Gamma'}{2}\right)\right]\sigma_{e_j,e_j} \\ &-i\hbar\frac{\sin(k_0 d)}{2k_0 d}\gamma_0\left(\sigma_+^{(1)}\sigma_-^{(2)} + \sigma_-^{(1)}\sigma_+^{(2)}\right), \end{aligned} \tag{5}$$

where $c_R^\dagger(x)$ $[c_L^\dagger(x)]$ is a bosonic operator creating a right-going (left-going) surface plasmon at x.

The eigenstate with energy matching the incoming plasmon $E_k = v_g k$ can be written as

$$|E_k\rangle = \int dx \left[\phi^+_{k,R}(x)c^\dagger_R(x) + \phi^+_{k,L}(x)c^\dagger_L(x)\right]|g_1,g_2\rangle\,|0\rangle_{\rm sp} + \sum_{j=1,2}\xi_{k_j}\sigma^{(j)}_+|g_1,g_2\rangle\,|0\rangle_{\rm sp}\,, \quad (6)$$

where ξ_{k_j} is the probability amplitude that the j-th QD absorbs the surface plasmon and jumps to its excited state, and $|g_1,g_2\rangle\,|0\rangle_{\rm sp}$ means that both, QD-1 and QD-2, are in their ground states with no SPs. For a single SP incident from the left, the scattering amplitudes $\phi^+_{k,R}(x)$ and $\phi^+_{k,L}(x)$ take the form

$$\begin{cases}\phi^+_{k,R}(x) \equiv \exp(ikx)\left[\theta(-x) + a\;\theta(x)\theta(d-x) + t\;\theta(x-d)\right],\\ \phi^+_{k,L}(x) \equiv \exp(-ikx)\left[r\;\theta(-x) + b\;\theta(x)\theta(d-x)\right],\end{cases} \quad (7)$$

where $\theta(x)$ is the unit step function which equals unity when $x \geq 0$ and zero when $x < 0$. Moreover, t and r are the transmission and reflection amplitudes, respectively, and $[a\;\exp(ikx)\theta(x)\theta(d-x)]$ and $[b\;\exp(-ikx)\theta(x)\theta(d-x)]$ represent the wavefunction of the SP between 0 and d. By solving the eigenvalue equation $H|E_k\rangle = E_k|E_k\rangle$, one can analytically obtain the reflection and transmission coefficients of single surface plasmon scattering[32,33]. Doing so we obtain the following relations for the coefficients

$$\begin{cases} g\left(2ae^{ikd} + 2be^{-ikd}\right) - \Gamma^{\rm SR}\;\xi_{k_1} = \left(\delta + \frac{i\Gamma'}{2}\right)\xi_{k_2},\\ g\left(1 + a + r + b\right) - \Gamma^{\rm SR}\;\xi_{k_2} = \left(\delta + \frac{i\Gamma'}{2}\right)\xi_{k_1},\\ a = 1 + \frac{g\xi_{k_1}}{iv_g},\;\; b = \frac{g\xi_{k_2}}{iv_g}\exp(ikd),\\ t = 1 + \frac{g}{iv_g}\left[\xi_{k_1} + \xi_{k_2}\exp(-ikd)\right],\\ r = \frac{g}{iv_g}\left[\xi_{k_1} + \xi_{k_2}\exp(ikd)\right],\end{cases} \quad (8)$$

The transmission and reflection amplitudes can then be determined algebraically. In the following discussion, we refer to the decay rate into surface plasmon modes as $\Gamma_{\rm pl} = 4\pi g^2/v_g$. This is convenient way to compare the strength of the plasmon-dot coupling and other decay channels.

A. Reflection and transmission of surface plasmons

First of all we analyze the reflection and transmission properties. Figure 2(a) numerically displays the transmission coefficient $T = |t|^2$ (dashed lines) and reflection coefficient $R = |r|^2$ (solid lines) for different values of the inter-dot distance d. The peak positions of the reflection coefficients sometimes deviate from the center ($\delta = 0$). Figure 2(c) shows the peak position as a function of kd. The continuous green (dotted blue) curve represents the result with (without) the super-radiant effect. As can be seen in Fig. 2(c), not only the interference from the inter-dot separation, but also the super-radiance affects the positions of the peaks. This is the only real contribution the super-radiance term makes to our results. Its effect on the entanglement, discussed in the next section, diminishes quickly as a function of d, thus we omit it completely in that treatment (see methods).

Figure 2(b) shows that the amplitude r of the reflection coefficient R is suppressed when increasing the non-radiative loss Γ_0. The inset in Fig. 2(b) is the scattering spectrum versus detuning δ of a single SP incident on two QDs with kd equal to an integer multiple of π. When $kd = 2n\pi$ $[(2n+1)\pi]$, with n being an integer, the phase difference of the SP between the two QDs is in-phase (π phase difference). This makes the two QDs collectively act like a single QD and results in a spectrum identical to the single QD case[33]. Note that the reflection coefficient $R(\delta)$ has one minimum when $\delta < 0$. Without the super-radiant effect, the positions of the minima, $\delta_{\rm min}$, can be deduced from Eq. (8) and satisfy the following relation:

$$-\tan^2(kd) = -4\left(\frac{\delta_{\rm min}}{\Gamma_{\rm pl}}\right)^2 - \left(\frac{\Gamma'}{\Gamma_{\rm pl}}\right)^2, \quad (9)$$

where $\Gamma_{\rm pl}$ is the QD exciton decay rate into SP modes, and $R(\delta_{\rm min}) = 0$. If there is no reflection ($r = 0$), one can say that Eq. (9) is the resonant tunneling condition for a photon traveling through two QDs. This $r = 0$ minimum can be seen close to $\delta = 0$ in Fig. 2(b). Note that our $R(\delta)$ and $T(\delta)$ are not symmetric around $\delta = 0$. This is because: (i) the incoming wave meets two scatterers, instead of one; and (ii) because we are considering the effects of super-radiance. Without the conditions (i) and (ii), (e.g., when $d = 0$) we would recover the Breit-Wigner scattering resulting in a symmetric Lorentzian, as opposed to the asymmetric forms we obtain for $R(\delta)$ and $T(\delta)$.

B. Entanglement generation

The transmitted or reflected SP propagating on the surface of the nanowire can, in principle, be observed by detectors placed at both ends of the nanowire[23]. Equations (1) and (2) oppositely imply that if there is no transmission or reflection SP detected at the two ends of the wire, the wavefunction is projected onto the state

$$\sum_{j=1,2}\xi_{k_j}\sigma^{(j)}_+|g_1,g_2\rangle\,|0\rangle_{\rm sp}\,. \quad (10)$$

This means that it is possible to create entanglement between the two dots. However, this projection, or post-selection, requires minimal Ohmic loss. This can be mitigated using the meta-stable states and waveguides discussed in the next section. Let us first consider the limit of $P \to \infty$ ($P \equiv \Gamma_{\rm pl}/\Gamma'$). Two special cases for achieving high entanglement are $kd = 2n\pi$ and $(2n+1)\pi$, for which the amplitude ξ_{k_1} is equal to ξ_{k_2} or $-\xi_{k_2}$, respectively. In this case, the two-dot qubits become triplet- or singlet-entangled if no surface plasmons are detected at the two ends of the wire.

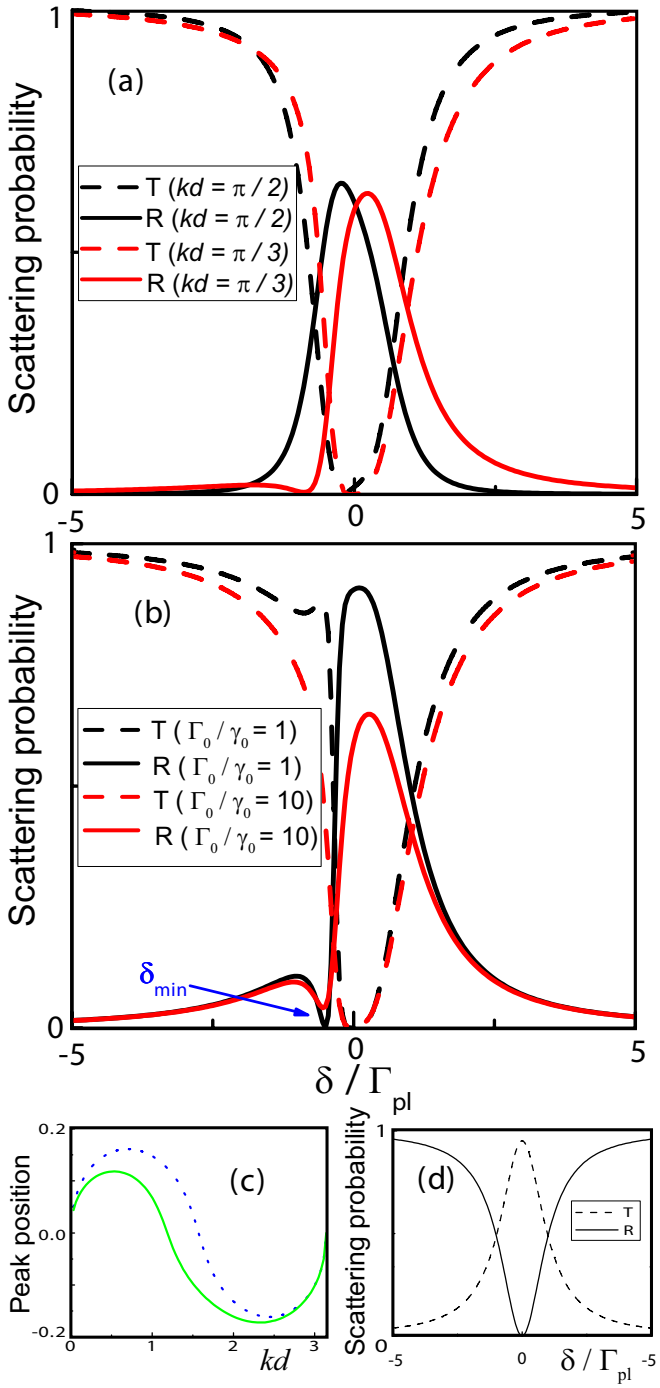

FIG. 2: (Color online) Transmission probabilities $T = |t|^2$ (dashed lines) and reflection probabilities $R = |r|^2$(solid lines) for a single surface plasmon scattered by two quantum dots, as a function of detuning $\delta = E_k/\hbar - \omega_0$. In the figures, γ_0 and Γ_0 are normalized to the decay rate into the surface-plasmon modes $\Gamma_{\rm pl}$, and we have chosen $\gamma_0 = \Gamma_0 = 0.025\Gamma_{\rm pl}$ in (a), and $kd = \pi/4$, $\gamma_0 = 0.025\Gamma_{\rm pl}$ in (b). (c) shows the peak positions of the reflection probabilities as a function of kd. The continuous green (dotted blue, top) curve represents the result with (without) the super-radiant effect. (d) refers to a surface plasmon incident on a single QD[33], which is also the case for two QDs with kd equal to a multiple of π.

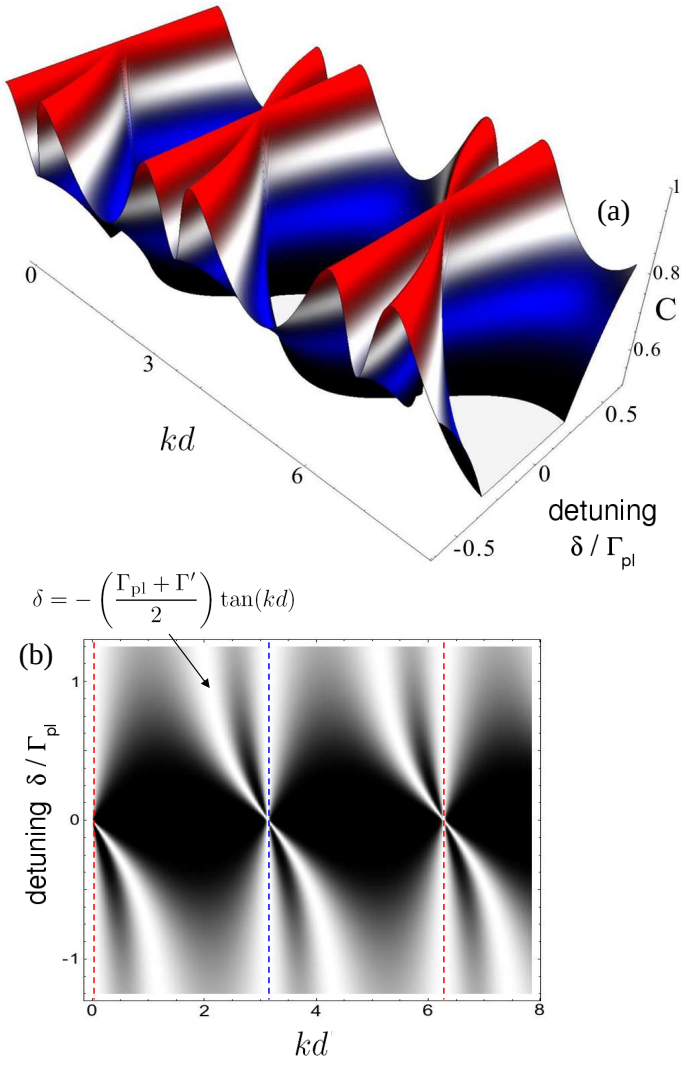

FIG. 3: (Color online) (a) Concurrence C of the two-dot qubits as functions of the inter-dot distance d and detuning δ in the limit $P \to \infty$. (b) shows the density plot of (a): the white regions correspond to high entanglement, with concurrence around 1. The red vertical dashed lines refer to $kd = 2n\pi$, while the blue vertical dashed line denotes the $kd = (2n+1)\pi$ case. Both of these conditions achieve high entanglement.

To demonstrate the degree of entanglement, Fig. 3 shows the concurrence[36] C of the two-dot qubits as functions of the inter-dot distance and detuning δ. The concurrence quantifies the degree of entanglement of two qubits. For our system, the density matrix of the two-dot state is a pure state density matrix, and the concurrence simply takes the form,

$$C = \frac{2|\xi_{k_1}| \cdot |\xi_{k_2}|}{|\xi_{k_1}|^2 + |\xi_{k_2}|^2}. \qquad (11)$$

The red dashed line in Fig. 3(b) refers to $kd = 2n\pi$, while the blue dashed line refers to $kd = (2n+1)\pi$. In addition to the special cases mentioned above, there are several

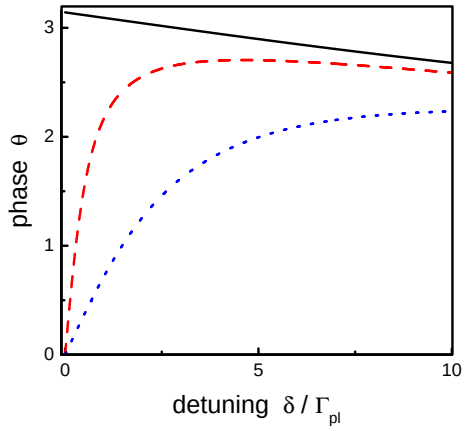

FIG. 4: (Color online) The phase factor θ of the entangled state $\xi_{k_1}|e_1, g_2\rangle + e^{i\theta} \cdot \xi_{k_2}|g_1, e_2\rangle$ in the limit of large d, when super-radiance is negligible. The continuous black (top), dashed red, and dotted blue (bottom) curves represent the results for $\Gamma' = 0$, $0.025\Gamma_{\rm pl}$, and $0.125\Gamma_{\rm pl}$, respectively.

curved "tangent-shaped" regions satisfying the condition of high entanglement, $C \approx 1$. In the limit of large d, we can neglect the effect of super-radiance and find that the equation of these curved regions are given by

$$\delta = -\left(\frac{\Gamma_{\rm pl} + \Gamma'}{2}\right) \tan(kd). \qquad (12)$$

The physical meaning of this condition is that even if the energy for the incident SP is not resonant with the qubit energy $\hbar\omega_0$, it is still possible to create a highly-entangled state, but only if the two dots are placed at the right locations. In this case, the entangled state now becomes $\xi_{k_1}|e_1, g_2\rangle + e^{i\theta} \cdot \xi_{k_2}|g_1, e_2\rangle$, i.e. there is an extra phase θ between $|e_1, g_2\rangle$ and $|g_1, e_2\rangle$.

Figure 4 shows the variations of the phase θ as a function of the detuning δ. In the limit of large d, there is no super-radiance and the continuous black (top), dashed red, and dotted blue (bottom) curves represent the results of $\Gamma' = 0$, $0.025\Gamma_{\rm pl}$, and $0.125\Gamma_{\rm pl}$, respectively. As can be seen in Fig. 4, once the dissipative loss Γ' is non-zero, the phase suddenly changes from π (top black line) to 0 (red and blue curves) when $\delta = 0$. However, the scattering treatment we use here does not truly reflect the dynamics of the coupled system: in reality, it takes a finite time for the plasmon to mediate the entanglement between the two dots. During this finite time, the entangled state will undergo decoherence, even if no plasmon is emitted to the left or right. Thus this "high entanglement" value will, in practice, be reduced (e.g., by emission of the QDs into other modes).

For finite Purcell factor P, the entanglement between the two QDs will be suppressed by the dissipation (Γ'). In the absence of further emission of a surface plasmon (e.g. because of ideal post-selection, or transfer to the metastable state, see next section) the entangled state will decay exponentially due to the losses into free space γ_0. This behavior is trivial, so we do not show it here. All of this implies the creation of the entangled state truly depends on $\Gamma_{\rm pl}$ dominating over the all decay channels (which is feasible[33]), and fast transfer of the entangled state into a metastable state. We discuss this in the next section.

III. ENTANGLEMENT STORAGE

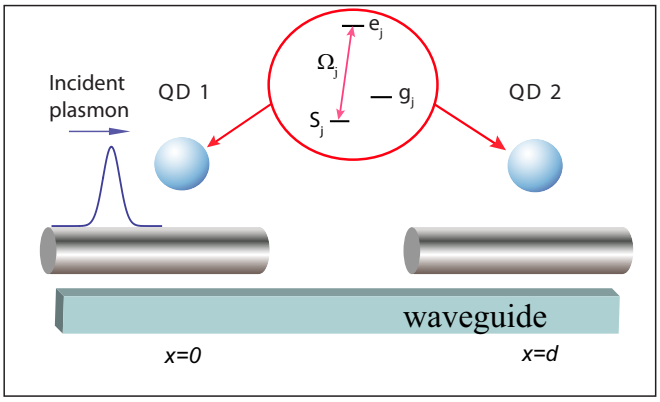

FIG. 5: (Color online) Schematic diagram of the storage process of the initial entangled state into metastable entangled states, $|s_1, g_2\rangle \pm |g_1, s_2\rangle$, with classical optical pulses $\Omega_1(t)$ and $\Omega_2(t)$. To avoid the possibility of strong losses in metal nano-wires, a dielectric waveguide is introduced to achieve remote entanglement. In the three-level diagram, the subscript j ($j = 1$ or 2) labels each QD.

One might argue that the entangled states created in this manner are fragile because the QDs are still coupled to the SPs. The entanglement would rapidly disappear either due to radiative or non-radiative losses or the SP would eventually escape and be detected (or lost during propagation in the nano-wire). The entangled state exists only on a very short time-scale. To overcome this, one can consider multilevel emitters, such as the three-level configuration[33] shown in Fig. 5. Metastable[37] states, $|s_1\rangle$ and $|s_2\rangle$, are decoupled from the SPs, but are resonantly coupled to $|e_1\rangle$ and $|e_2\rangle$, respectively, via a classical optical control field with Rabi frequencies $\Omega_1(t)$ and $\Omega_2(t)$. Here, the metastable states mean that the relaxation times of the states $|s_1\rangle$ and $|s_2\rangle$ are much longer than that of the excited states $|e_1\rangle$ and $|e_2\rangle$.

Three remarks about experimental realizations should be addressed here. First, for the realization of the coupling between a metal nanowire SP and the two QDs, colloidal CdSe/ZnS QDs and a silver nanowire are ideal since the exciton energy of CdSe/ZnS QDs is around 2-2.5 eV, compatible with the saturation plasma energy[23] (≈ 2.66 eV) of the silver nanowire.

Second, the SPs inevitably experience losses as they propagate along the nanowire, which limits the feasibility of creating remote entanglement. One solution to this problem would be to couple the two dots to two separate nanowires, as shown in Fig. 5. Also, the wires

are evanescently coupled to a phase-matched dielectric waveguide[33,38]. In this case, one can have both the advantages of strong coupling to the SPs, and long-distance transport through the dielectric waveguide.

Third, once the entangled state has been prepared, how can it be detected? One possible procedure is to use ultra-fast optical tomography as outlined in Ref. [39]. This would allow one to reconstruct the density matrix of the effective two-dot (qubit) system (which in practice will be a mixed state due to environmental effects, and the inevitable decay of the meta-stable states), and consequently obtain the concurrence of the two dots.

IV. SUMMARY AND CONCLUSIONS

In summary, we have examined the scattering properties of the SPs in a metal nanowire coupled with two QDs. Both the dissipative losses and the super-radiant effect are found to influence the scattering properties. We then used this system to propose a scheme to create a remote entangled state between the two QDs. Using metastable states and waveguides this might be possible even in the presence of metal and radiative losses. In future work one could consider how the presence of entanglement could be tested with the Bell Inequality by scattering another plasmon off the entangled two-dot state and performing measurements akin to those proposed for edge states in quantum Hall systems[40]. In addition, this proposal can also be applied to other physical systems. For example, one can easily extend this to photons (e.g., in transmission lines or waveguides) coupled to artificial atoms (e.g., superconducting qubit)[32,41,42].

Acknowledgments

This work is supported partially by the National Science Council, Taiwan, under the grant number NSC 98-2112-M-006-002-MY3. G.Y.C. and Y.N.C. acknowledge A. Buchleitner, F. Mintert, C. M. Li, and J. R. Johansson for helpful discussions. N.L. is supported by RIKEN's FPR scheme. F.N. acknowledges partial support from the Laboratory of Physical Sciences, National Security Agency, Army Research Office, Defense Advanced Research Projects Agency, Air Force Office of Scientific Research, National Science Foundation Grant No. 0726909, JSPS-RFBR Contract No. 09-02-92114, Grant-in-Aid for Scientific Research (S), MEXT Kakenhi on Quantum Cybernetics, and Funding Program for Innovative R&D on S&T (FIRST).

V. APPENDIX

A. Super-radiant decay

The inclusion of the super-radiant term in the non-Hermitian form can be justified as follows. One can start with a master equation for the two QDs coupled to external modes or with a simple application of Fermi's Golden rule (e.g., as in Ref. [43]). In the singlet, $|S\rangle = \frac{1}{\sqrt{2}}(|e_1, g_2\rangle - |g_1, e_2\rangle)$, and triplet, $|T\rangle = \frac{1}{\sqrt{2}}(|e_1, g_2\rangle + |g_1, e_2\rangle$, bases this master equation has several super-radiant and sub-radiant decay terms, describing the following decay channels: via rate Γ_+ for the channel $T_+ \to T \to T_-$; and via the rate Γ_- for the channel $T_+ \to S \to T_-$. Since we omit the double-occupation terms here, only the channels from S and T contribute. These give the following Lindblad terms in the master equation for the density matrix of the two dots[34,43],

$$\begin{aligned} L_+ &= -\frac{\Gamma_+}{2}\Big(|T\rangle\langle T|\rho + \rho|T\rangle\langle T| - |T_-\rangle\langle T|\rho|T\rangle\langle T_-|\Big), \\ L_- &= -\frac{\Gamma_-}{2}\Big(|S\rangle\langle S|\rho + \rho|S\rangle\langle S| - |T_-\rangle\langle S|\rho|S\rangle\langle T_-|\Big). \end{aligned} \tag{13}$$

Where

$$\Gamma_\pm = \gamma_0\left[1 \pm \frac{\sin(k_0 d)}{k_0 d}\right]. \tag{14}$$

For both L_- and L_+, the first two terms contribute to the non-hermitian Hamiltonian, while the last term is the "quantum jump" term. As mentioned above, these jump terms can be neglected in here because a loss of excitation from either quantum dot means a loss of the input SP. Combining the other terms, and rewriting the singlet and triplet bases in the dot excitation basis, gives the following contribution to the effective non-Hermitian Hamiltonian,

$$\begin{aligned} H_{\rm eff}^{\rm SR} &= -i\hbar\frac{\gamma_0}{2}\left(\sigma_{e_1,e_1} + \sigma_{e_2,e_2}\right) \\ &- i\hbar\frac{\sin(k_0 d)}{2k_0 d}\gamma_0\left(\sigma_+^{(1)}\sigma_-^{(2)} + \sigma_-^{(1)}\sigma_+^{(2)}\right) \end{aligned} \tag{15}$$

B. ENTANGLEMENT STORAGE

For the entanglement storage process, instead of transforming Eq. (1) into real space, we represent the Hamiltonian under the bases of singlet, $|S\rangle = \frac{1}{\sqrt{2}}(|e_1, g_2\rangle - |g_1, e_2\rangle)$, and triplet, $|T\rangle = \frac{1}{\sqrt{2}}(|e_1, g_2\rangle + |g_1, e_2\rangle$, states:

$$
\begin{aligned}
H &= \hbar\left(\omega_0 - i\frac{\Gamma'}{2}\right)\left(|T\rangle\langle T| + |S\rangle\langle S|\right) \\
&\quad -\hbar g\int dk\ \left\{\left[\frac{1}{\sqrt{2}}\left(1+e^{ikd}\right)|T\rangle\langle g_1,g_2|\,a_k\right.\right. \\
&\quad \left.\left.+\frac{1}{\sqrt{2}}\left(1-e^{ikd}\right)|S\rangle\langle g_1,g_2|\,a_k\right] + \text{h.c.}\right\} \\
&\quad +\int dk\ \hbar v_{\rm g}|k|a_k^\dagger a_k, \qquad (16)
\end{aligned}
$$

where we have adopted the approximation that the superradiant effect can be neglected in the limit of large d. We now consider the general time-dependent wave function

$$
\begin{aligned}
|\psi\rangle &= \int dk[c_{R,k}(t)\hat{a}^\dagger_{R,k} + c_{L,-k}(t)\hat{a}^\dagger_{L,-k}]\,|g_1,g_2;0\rangle \\
&\quad +c_T(t)\,|T;0\rangle + c_S(t)\,|S;0\rangle \qquad (17)\\
&\quad +c_{M_T}(t)\,|M_T;0\rangle + c_{M_S}(t)\,|M_S;0\rangle\,,
\end{aligned}
$$

where $|M_S\rangle = \frac{1}{\sqrt{2}}(|s_1,g_2\rangle - |g_1,s_2\rangle)$ and, $|M_T\rangle = \frac{1}{\sqrt{2}}(|s_1,g_2\rangle + |g_1,s_2\rangle)$, denote the singlet and triplet metastable states, respectively. From $H\,|\psi\rangle = i\hbar\partial_t\,|\psi\rangle$, the state amplitudes evolve according to

$$
\begin{aligned}
\frac{d\ c(t)}{dt} &= -i\delta_k c(t) + \frac{ig}{\sqrt{2}}(1+e^{-ikd})c_T(t) \\
&\quad +\frac{ig}{\sqrt{2}}(1-e^{-ikd})c_S(t), \qquad (18)
\end{aligned}
$$

where $\delta_k = v_{\rm g}k - \omega_0$. The equation above refers to, in a compact manner, to two equations: one for $c_{R,k}$ and the other one for $c_{L,-k}$, respectively. If $\Omega_1(t) = \Omega_2(t)$ and $kd = 2n\pi$, Eq. (16) can be substituted into the equation of motion for $c_T(t)$

$$
\begin{aligned}
\frac{d\ c_T(t)}{dt} &= -\frac{\Gamma'}{2}c_T(t) + i\Omega_1(t)c_{M_T}(t) \\
&\quad +ig\int dk[c_{R,k}(t) + c_{L,-k}(t)], \qquad (19)
\end{aligned}
$$

which yields an integro-differential equation involving $c_T(t)$. Imposing the reasonable constraint that the SP storage process has no outgoing field at the end of the wire, such that $c_{R,k(L,-k)}(\infty) = 0$, one can obtain an implicit expression for the required pulse shape $\Omega_1(t)$ and the following equation related to the population in the state $|M_T\rangle$

$$
\frac{d}{dt}\,|c_{M_T}(t)|^2 = \frac{-v_{\rm g}^2}{2\pi g^2}\left(\frac{d}{dt}\,|E_T(t)|^2 - \frac{\Gamma_{pl}-\Gamma'}{2}\,|E_T(t)|^2\right), \qquad (20)
$$

where

$$
E_T(t) = -\sqrt{2\pi}ig c_T(t)/v_{\rm g}. \qquad (21)
$$

With the normalization condition,

$$
\int_{-\infty}^{\infty} dt\,|E_T(t)|^2 = 1/(2v_{\rm g}), \qquad (22)
$$

and assuming that the incoming field vanishes[33] at $t = \pm\infty$ [i.e., $E_T(\pm\infty) = 0$], Eq. (17) can be integrated to yield

$$
|c_{M_T}(\pm\infty)|^2 = 1 - 1/P, \qquad (23)
$$

where

$$
P \equiv \Gamma_{\rm pl}/\Gamma', \qquad (24)
$$

is the effective Purcell factor. Similarly, it can be easily shown that the storage efficiency into the $|M_S\rangle$ state is also equal to $1 - 1/P$, if $\Omega_1(t) = -\Omega_2(t)$ and $kd = (2n+1)\pi$. Note that the metal and radiative losses on the qubits are taken into account in the above derivation. Therefore, the entangled states can be stored with a high efficiency only if the Purcell factor P is large enough. Furthermore, the two qubits could be separated far away from each other, such that one can address one qubit without affecting the other.

* Electronic address: yuehnan@mail.ncku.edu.tw

[1] G. Kostantatos, and E. H. Sargent, Nanostructured materials for photon detection, *Nature Nanotechnology* **5**, 391-400 (2010).

[2] R. Zia, M. L. Brongersma, Surface plasmon polariton analogue to Young's double-slit experiment, *Nature Nanotechnology* **2**, 426-429 (2007).

[3] K. Yu. Bliokh, Yu. P. Bliokh, V. Freilikher, S. Savel'ev, and F. Nori, Colloquium: Unusual resonators: Plasmonics, metamaterials, and random media, *Rev. Mod. Phys.* **80**, 1201-1213 (2008).

[4] S. Savel'ev, V. A. Yampol'skii, A. L. Rakhmanov, F. Nori, Terahertz Josephson plasma waves in layered superconductors: spectrum, generation, nonlinear, and quantum phenomena, *Rep. Prog. Phys.* **73**, 026501 (2010).

[5] W. L. Barnes, A. Dereux, T. W. Ebbesen, Surface plasmon subwavelength optics, *Nature* **424**, 824-830 (2003).

[6] D. K. Gramotnev, and S. I. Bozhevolnyi, Plasmonic beyond the diffraction limit, *Nature Photonics* **4**, 83-91 (2010).

[7] S. I. Bozhevolnyi, V. S. Volkov, E. Devaux, J. Laluet, and T. W. Ebbesen, Channel plasmon subwavelength waveguide components including interferometers and ring resonators, *Nature* **440**, 508-511 (2006).

[8] D. E. Gómez, K. C. Vernon, P. Mulvaney, and T. J. Davis, Surface plasmon mediated strong exciton-photon coupling in semiconductor nanocrystals, *Nano Lett.* **10**, 274-278 (2009).

[9] C. -C. Chang, Y. D. Sharma, Y. -S. Kim, J. A. Bur, R. V. Shenoi, S. Krishna, D. Huang, and S. -Y. Lin, A surface plasmon enhanced infrared photodetector based on InAs quantum dots, *Nano Lett.* **10**, 1704-1709 (2010).

[10] E. Hwang, I. I. Smolyaninov, and C. C. Davis, Surface plasmon polariton enhanced fluorescence from quantum-dots on nanostructured metal surfaces, *Nano Lett.* **10**, 10, 813-820 (2010).

[11] H. Gao, J. Henzie, and T. W. Odom, Direct evidence for surface plasmon-mediated enhanced light transmission through metallic nanohole arrays, *Nano Lett.* **6**, 2104-2108 (2006).

[12] D. Pacifici, H. J. Lezec, and H. A. Atwater, All-optical modulation by plasmonic excitation of CdSe quantum dots, *Nature Photonics* **1**, 402-406 (2007).

[13] P. Zijlstra, J. W. M. Chon, and M. Gu, Five-dimensional optical recording mediated by surface plasmons in gold nanorods. *Nature* **459**, 410-413 (2009).

[14] B. Dragnea, J. M. Szarko, S. Kowarik, T. Weimann, J. Feldmann, and S. R. Leone, Near-field surface plasmon excitation on structured gold films, *Nano Lett.* **3**, 3-7 (2003).

[15] J. Stolze and D. Suter, Quantum Computing (Wiley-VCH, Weinheim, 2008); W. P. Schleich and H. Walther (Eds), Elements of Quantum Information (Wiley-VCH, Weinheim, 2008).

[16] A. T. Costa and S. Bose, Impurity scattering induced entanglement of ballistic electrons, *Phys. Rev. Lett.* **87**, 277901 (2001).

[17] W. D. Oliver, F. Yamaguchi, and Y. Yamamoto, Electron entanglement via a quantum dot, *Phys. Rev. Lett.* **88**, 037901 (2002).

[18] O. Gywat, G. Burkard, and D. Loss, Biexcitons in coupled quantum dots as a source of entangled photons, *Phys. Rev. B* **65**, 205329 (2002).

[19] J. Q. You, and F. Nori, Superconducting circuits and quantum information, Physics Today **58**, 42-47 (2005).

[20] A. J. Berkley, H. Xu, R. C. Ramos, M. A. Gubrud, F. W. Strauch, P. P. Johnson, J. R. Anderson, A. J. Dragt, C. J. Lobb, and F. C. Wellstood, Entangled macroscopic quantum states in two superconducting qubits, *Science* **300**, 1548-1550 (2003).

[21] M. Steffen, M. Ansmann, R. C. Bialczak, N. Katz, E. Lucero, R. McDermott, M. Neeley, E. M. Weig; A. N.Cleland, and J. M. Martinis, Measurement of the entanglement of two superconducting qubits via state tomography, *Science* **313**, 1423-1425 (2006).

[22] J. Majer, J. M. Chow, J. M Gambetta, J. Koch, B. R. Johnson, J. A. Schreier, L. Frunzio, D. I. Schuster, A. A. Houck, A. Wallraff, A. Blais, M. H. Devoret, S. M. Girvin, and R. J. Schoelkopf, Coupling Superconducting Qubits via a Cavity Bus, *Nature* **449**, 443-447 (2007).

[23] A. V. Akimov, A. Mukherjee, C. L. Yu, D. E. Chang, A. S. Zibrov, P. R. Hemmer, H. Park, and M. D. Lukin, Generation of single optical plasmons in metallic nanowires coupled to quantum dots, *Nature* **450**, 402-406 (2007).

[24] J. -T. Shen, and S. Fan, Theory of single-photon transport in a single-mode waveguide. I. Coupling to a cavity containing a two-level atom, *Phys. Rev. A* **79**, 023837 (2009).

[25] W. Chen, G. Y. Chen, and Y. N. Chen, Coherent transport of nanowire surface plasmons coupled to quantum dots, *Opt. Express* **18**, 10360 (2010).

[26] A. Gonzalez-Tudela, D. Martin-Cano, E. Moreno, L. Martin-Moreno, C. Tejedor, and F. J. Garcia-Vidal, Entanglement of two qubits mediated by one-dimensional plasmonic waveguides, *Phys. Rev. Lett.* **106**, 020501 (2011).

[27] D. Martin-Cano, L. Martin-Moreno, F. J. Garcia-Vidal, and E. Moreno, Resonance energy transfer and superradiance mediated by plasmonic nanowaveguides, *Nano Lett.* **10**, 10, 3129-3134 (2010).

[28] D. E. Chang, A. S. Sørensen, P. R. Hemmer, and M. D. Lukin, Quantum optics with surface plasmons , *Phys. Rev. Lett.* **97**, 053002 (2006).

[29] G. Y. Chen, Y. N. Chen, and D. S. Chuu, Spontaneous emission of quantum dot excitons into surface plasmons in a nanowire, *Opt. Lett.* **33**, 2212-2214 (2008).

[30] D. Dzsotjan, A. S. Sørensen, and M. Fleischauer, Quantum emitters coupled to surface plasmons of a nanowire: A Green's function approach, *Phys. Rev. B* **82**, 075427 (2010).

[31] G. Khitrova, H. M. Gibbs, M. Kira, S. W. Koch, and A. Scherer, Vacuum Rabi splitting in semiconductors, *Nature Physics* **2**, 81-90 (2006).

[32] J. -T. Shen, and S. Fan, Coherent Single Photon Transport in a One-Dimensional Waveguide Coupled with Superconducting Quantum Bits, *Phys. Rev. Lett.* **95**, 213001 (2005).

[33] D. E. Chang, A. S. Sørensen, E. A. Demler, M. D. Lukin, A single-photon transistor using nanoscale surface plasmons, *Nature Physics* **3**, 807-812 (2007).

[34] Y. N. Chen, D. S. Chuu, and T. Brandes, Current detection of superradiance and induced entanglement of double quantum dot excitons, *Phys. Rev. Lett.* **90**, 166802 (2003); N. Lambert, Y. N. Chen, J. R. Johansson, F. Nori, Quantum chaos and critical behavior on a chip, Phys. Rev. B

80, 165308 (2009).

[35] P. Meystre and M. Sargent III, Elements of Quantum Optics 3rd ed. (Springer, New York, 1999).

[36] W. K. Wootters, Entanglement of formation of an arbitrary state of two qubits, *Phys. Rev. Lett.* **80**, 2245-2248 (1998).

[37] M. Orrit, Photons pushed together, *Nature* **460**, 42-44 (2009); J. Hwang, M. Pototschnig, R. Lettow, G. Zumofen, A. Renn, S. Götzinger, and V. Sandoghdar, A single-molecule optical transistor, *Nature* **460**, 76-80 (2009); F. Dubin, C. Russo, H. G. Barros, A. Stute, C. Becher, P. O. Schmidt, and R. Blatt, Quantum to classical transition in a single-ion laser, *Nature Physics* **6**, 350-353 (2010).

[38] B. Dayan, A. S. Parkins, T. Aoki, E. P. Ostby, K. J. Vahala, and H. J. Kimble, A photon turnstile dynamically regulated by one atom, *Science* **319**, 1062 (2008).

[39] Y. Wu, X. Li, L. M. Duan, D. G. Steel, and D. Gammon, Density matrix tomography through sequential coherent optical rotations of an exciton Qubit in a Single Quantum Dot, *Phys. Rev. Lett.* **96**, 087402 (2006).

[40] C. W. J. Beenakker, C. Emary, M. Kindermann, and J. L. van Velsen, Proposal for Production and Detection of Entangled Electron-Hole Pairs in a Degenerate Electron Gas, *Phys. Rev. Lett.* **91**, 147901 (2003).

[41] L. Zhou, Z. R. Gong, Y. X. Liu, C. P. Sun, and F. Nori, Controllable Scattering of a Single Photon inside a One-Dimensional Resonator Waveguide , *Phys. Rev. Lett.* **101**, 100501 (2008); L. Zhou, S. Yang, Y. X. Liu, C. P. Sun, and F. Nori, Quantum Zeno switch for single-photon coherent transport, *Phys. Rev. A* **80**, 062109 (2009); L. Zhou, H. Dong, Y. X. Liu, C. P. Sun, and F. Nori, Quantum super-cavity with atomic mirrors, *Phys. Rev. A* **78**, 063827 (2008); J. Q. Liao, Z. R. Gong, L. Zhou, Y. X. Liu, C. P. Sun, and F. Nori, Controlling the transport of single photons by tuning the frequency of either one or two cavities in an array of coupled cavities, *Phys. Rev. A* **81**, 042304 (2010).

[42] S. Fan, Ş. E. Kocabaş, and J. -T. Shen, Input-output formalism for few-photon transport in one-dimensional nanophotonic waveguides coupled to a qubit, *Phys. Rev. A* **82**, 063821 (2010).

[43] R. G. DeVoe, and R. G. Brewer, Observation of superradiant and subradiant spontaneous emission of two trapped ions, *Phys. Rev. Lett.* **76**, 2049 (1996).